Electronic Supplementary Material (ESI) for Soft Matter.

Two-component Charge Transfer Hydrogel with Excellent Multi-Stimuli Responsive Behavior: A Platform to Differentiate Different Biological Thiols

Dipen Biswakarma,[a] Nilanjan Dey [a] and Santanu Bhattacharya *[a,b]

[a]Department of Organic Chemistry, Indian Institute of Science, Bangalore, Karnataka 560012, India

[b]School of Applied & Interdisciplinary Sciences, Indian Association for the Cultivation of Science, Jadavpur, Kolkata 700 032, India

Email: sb@iisc.ac.in

Physical measurements and instrumentation

Material and Methods. All chemicals, solvents and silica gel for TLC were obtained from well-known commercial sources and were used without further purification, as appropriate. Solvents were distilled and dried by standard procedure before use. Melting points was measured in open capillaries and were uncorrected. ^{1}H-NMR and ^{13}C-NMR spectra were recorded in Bruker-400 Advance NMR spectrometer. Chemical shifts were reported in ppm downfield from the internal standard tetramethyl silane (TMS). Mass spectrometry of individual compounds was performed using a Micro Mass ESI-TOF MS instrument. Elemental analysis was recorded in Thermo Finnigan EA FLASH 1112 SERIES.

Gelation Studies. A detailed procedure of gelation has been discussed in the main manuscript. The formation of the gel was confirmed using the tube inversion method. In typical experiment **PyHisOH** and **NBD-Ox** was weight and was mixed in 1:1 molar ration. To this mixture PBS buffer (10 mM, pH 7.4 were prepared in deionized water and the pH solutions were obtained by the adjustment of PBS buffer solution with 1 mM HCl or 1 mM NaOH) was added followed by heating at 80 ºC till the solution became transparent. The resultant solution was sonicated for a few minutes subsequently allowed them to cool at room temperature. If a gel was formed, it was evaluated quantitatively by determining the critical gelator concentration (CGC) which is the minimum amount of gelator required to immobilize 1 mL of a particular solvent or solvent mixtures. A glass tube with a capacity of 10 x 75 mm has been used for the CGC measurement and CGC of the charge transfer hydrogel is 0.75 mM. For thixotropic property the CT gel was vortexed for 30 sec for complete gel-to sol transition and kept at rest for 10 mins to revert to gel.

FT-IR Spectroscopy. Prepared solution and gels were drop casted on the CaF_2 cell and dried under vacuum and FT-IR spectra were recorded in Perkin Elmer Spectrum BX FT-IR system. For the solid sample we have taken the powder sample and then FT-IT was recorded.

UV/Vis and Fluorescence Spectroscopy. The UV-Vis Spectroscopy and Fluorescence Spectroscopy of described solutions/suspensions were recorded on a Shimadzu model 2100 spectrophotometer and Cary-Eclipse spectrofluorimeter respectively, both equipped with a temperature controller bath. The slit width for the fluorescence experiment was kept at 5 nm

(excitation) and 5 nm (emission) and the excitation wavelength was set at 345 nm for **PyHisOH** and 385 nm for **NBD-Ox**.

Circular Dichroism Spectroscopy (CD). All the CD spectra of described solutions were recorded on a JASCO instrument, Model J-815-150S. Experiments were performed by purging dry N_2 gas continuously. Data were collected in a quartz cuvette of 1 mm path length between 200 to 450 nm.

Atomic Force Microscopy (AFM). Hydrogels were prepared in pH 7.4 solutions at a fixed concentration and were aged for 25 minutes at 27 °C**.** A dilute solution of the sample so prepared was deposited on freshly cleaved mica surface and then carefully air-dried. Each of the samples was analyzed using a JPK 00901 AFM instrument and Nano-Wizard software. Tapping mode off 10 nm tip radius, silicon tip, 292 KHz resonant frequency, 0.7-1 Hz scan speed, 256 x 256 and 512 x 512- pixels.

Scanning Electron Microscopy (SEM). Hydrogels were prepared in pH 7.4 solutions at a fixed concentration and were aged for 25 minutes at 27 °C. The gels of these specified solution were carefully drop casted onto the brass stubs and were allowed to air-dry overnight. The samples were then coated with gold vapor and analyzed on a Quanta 200 SEM operated at 10-15 kV.

X-ray Diffraction. The gel sample of the specified concentration was prepared and was carefully taken on glass slide and dried under vacuum for the corresponding XRD measurement. These samples were examined using Bruker D8 Advance instrument (θ, 2θ geometry with Scintillation Detectors). The X- ray beam generated with a rotating Cu anode at the wavelength of KR beam at 1.5418 was directed towards the film directed toward the film edge and scanning was done up to a 2θ value of 30°. Data were then analyzed and interpreted using the Bragg equation.

Energy Minimization. Energy minimization of the compound was performed using B3LYP/6-31G* level of computations.[Sd-e]

Rheological studies. Rheology experiments of the gels were carried out using Antor Paar MCR 52 with a cone and plate geometry (CP 25-2) having an adjustable peltier temperature controlling system. The distance between the cone and plates was kept fixed at 0.105 mm for all the measurement. The gels were taken on the plate of the rheometer. An oscillatory strain amplitude sweep experiment was performed at a constant oscillation frequency of 1 Hz for the

applied strain range 0.01-100 % at 20 °C. The rheometer has inbuilt software that converts the torque measurements into either G' (the storage modulus) and G" (the loss modulus) which is represented either as strain or shear stress. Oscillatory frequency sweep experiments were performed in the linear viscoelastic region (strain 0.01%) to ensure that calculated parameters correspond to an intact network structure.

Fluorescence-Decay Experiments. Fluorescence lifetimes were measured by using a time-correlated single-photon-counting fluorimeter (Horiba Jobin Yvon). The system was excited with nano LED light (Horiba–Jobin Yvon) with a pulse duration of 1.2 ns. (slit width: 2/2, λ_{em}=345 nm). The average fluorescence lifetimes (τ_{av}) for the exponential iterative fitting were calculated from the decay times (τ_i) and the relative amplitudes (α_i) by using Equation (1), where a_1-$_3$ are the relative amplitudes and τ_{1-3} are the lifetime values.

$$\tau_{av} = (\alpha_1\tau_1^2 + \alpha_2\tau_2^2 + \alpha_3\tau_3^2)/(\alpha_1\tau_1 + \alpha_2\tau_2 + \alpha_3\tau_3)$$

Synthesis and Characterization

The syntheses of the compounds **PyHisOMe**, **PyTyrOH**, **PyTrpOH**, and **PyPheOH** were carried out according to previously reported procedures.[Sa-b] Synthetic scheme of **PyHisOH** and **NBD-Ox** is shown below.

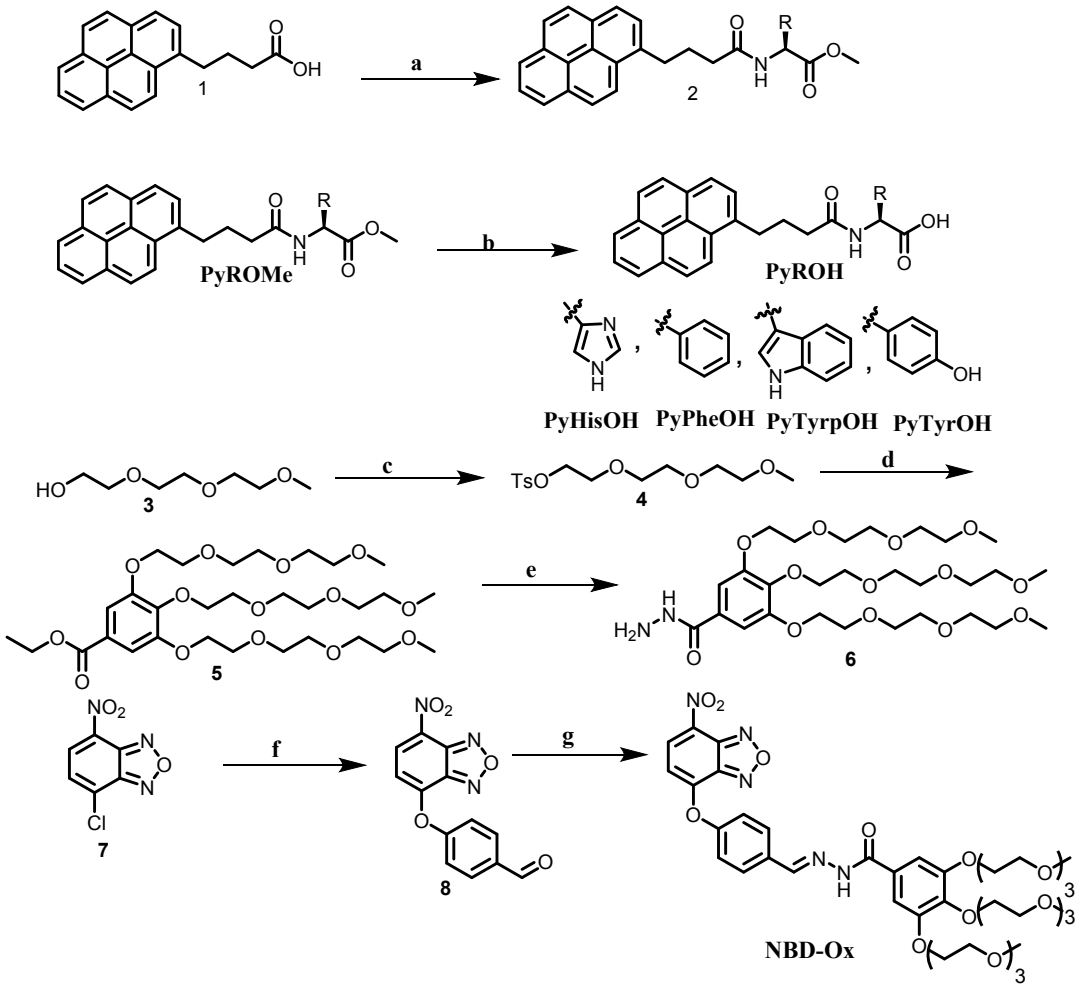

Reagents, reaction conditions, and yields: (a) L-aminoacid methyl ester .HCl, DCC, HOBt, 0 °C- rt, 24 h, 85%; (b) MeOH , 1M NaOH, 10 h, rt, 95 % ; (c) NaOH, H_2O, TsCl, 6 h, rt, 98%; (d) Ethyl gallate, K_2CO_3, DMF, 80 °C, 48 h, 75%; (e) $NH_2NH_2.H_2O$, MeOH, 65 °C, 24 h 96%; (f) p-hydroxybenzaldehyde, KOAc, EtOH , 20 mins, 87%;(g) **6**, EtOH , reflux, 3 h, 79%.

Synthesis of PyHisOH: The compound **PyHisOMe** was synthesized according to earlier reported procedure[Sb]. **PyHisOMe** (2 g, 4.55 mmol) so obtained was then dissolved in MeOH followed by the addition of 1M NaOH (7 mL) to it. The resultant mixture was then stirred, and the progress of the reaction was monitored using thin layer chromatography (TLC). After 12 h reaction mixture was removed, and the methanol was evaporated using a vacuum. The residue

so obtained was taken in 40 mL water and it was washed using diethyl ether twice, 1M HCl was used to adjust the pH of the aqueous solution to 2.0. The aqueous layer was then extracted using ethyl acetate. The solvent was evaporated using a vacuum to give off white solid product with 90.6 % yield. m.p.184 °C, IR (Neat cm^{-1}) IR (Neat, cm^{-1}) 3421, 3326, 3065, 2679, 1721, 1642, 1461, 1167, 1018; ^{1}H NMR (400 MHz, DMSO-d_6): δ 1.94-1.98 (m, 2H), 2.25-2.27 (m, 2H), 2.90-3.04 (m, 1H), 3.14-3.18(m, 1H), 3.24-3.28 (m, 2H), 4.59-4.64 (m, 1H), 7.39 (s, 1H), 7.89-7.91 (d, *J* = 7.8 Hz, 1H), 8.04-8.08 (t, *J* = 7.52 Hz, 1H), 8.13-8.23 (m, 2H), 8.26-8.29 (m, 4H), 8.33-8.39 (m, 2H), 8.94 (s, 1H) ;^{13} C NMR (100 MHz, DMSO-d_6) : δ 27.23, 28.35, 32.97, 35.63, 52.06, 117.76, 124.40, 125.06, 125.14, 125.72, 125.86, 127.07, 127.44, 128.17, 128.36, 128.46, 129.05, 130.66, 131.34, 134.67, 137.42, 173.12, 172.19; HRMS: *m/z* calcd. for CHNO (M + H^+) 462.1794, found: 462.1796; Elem. Anal.: calcd for CHNO C 73.39; H 5.45; N 9.88; found C 73.52; H 5.4619; N 9.4357.

Synthesis of 6 and 8: 6 and **8** was synthesised using reported procedure in the literature.[Sb-c]

Synthesis of NBD-Ox: NBD-Ox: A mixture of **6** (1 g, 1.56 mmol) and **8** (0.45 g, 1.56 mmol) was taken in a round bottom flask and to it EtOH (25 mL) was added. The resulting mixture was refluxed for 12 h under a nitrogen atmosphere and then cooled to room temperature. The reaction mixture was concentrated by evaporating the EtOH using a high vacuum and the crude product was purified by silica gel column chromatography using 3-4 % MeOH/$CHCl_3$ to give brown viscous liquid with 78% yield. m.p. 175 °C; IR (Neat, cm^{-1}) 2928, 1643, 1539, 1373, 1330; ^{1}H NMR (400 MHz, DMSO-d_6) δ 3.33 (m, 9H), 3.42 (m, 6H), 3.50-3.62 (m, 18H), 3.67-3.78 (m, 6H), 4.09-4.19 (m, 6H), 6.83-6.85 (d, *J* = 8.4 Hz, 1H), 7.23-7.52 (s, 2H), 7.51-7.53 (d, *J* = 8.4 Hz, 2H), 7.93-7.95 (d, *J* = 8.4 Hz, 2H), 8.53 (s, 1H), 8.66-8.68 (d, *J* = 8.4 Hz, 1H), 11.7 (s, 1H); ^{13}C NMR (100 MHz, $CDCl_3$) δ 58.91, 68.89, 69.65, 70.30, 70.47, 71.82, 72.27, 108.31, 115.63, 116.24, 118.18, 121.06, 128.18, 129.86, 130.89, 133.47, 141.42, 144.17, 145.14, 146.98, 152.20, 153.94, 163.87; HRMS: *m/z* calcd. for $C_{41}H_{55}N_5O_{17}$ $(M + Na)^+$: 912.3491, found: 912.3495; Elem. Anal.: calcd. for $C_{41}H_{55}N_5O_{17}$: C, 55.03; H, 6.37; N, 7.50; found: C, 56.74; H, 5.48; N, 7.14.

References:

Sa. J. Nanda, A. Biswas and A. Banerjee, *Soft Matter*, 2013, **9**, 4198-4208.

Sb. S. Bhattacharjee, B. Maiti and S. Bhattacharya, *Nanoscale*, 2016, **8**, 11224–11233.

Sc. U. Kessler, D. Castagnolo, M. Pagano, D. Deodato, M. Bernardini, B. Pilger, C. Ranadheera and M. Botta, *Bioorg. Med. Chem. Lett.* 2013, **23**, 5575-5577.

Sd. N. Dey, S.K. Samanta, and S. Bhattacharya, *ACS Appl. Mater. Interfaces* 2013, **5**, 8394−8400.

Se. S. Datta and S. Bhattacharya, *Chem. Commun.,* 2012, **48**, 877–879.

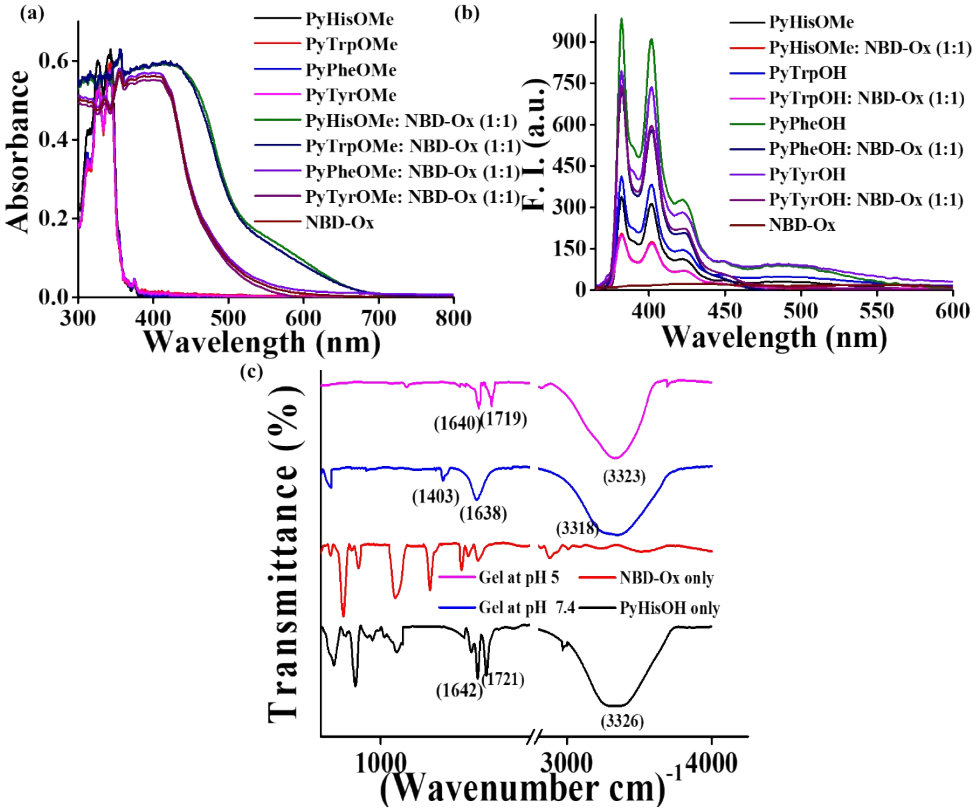

Figure S1. (a) Absorption and (b) emission spectra (λ_{ex} = 345 nm) showing the 1:1 charge transfer interaction between different donors and **NBD-Ox** in PBS buffer of pH 7.4. (c) FT-IR spectra of CT hydrogel (at pH 7.4 and 5), donor and acceptor.

(a)

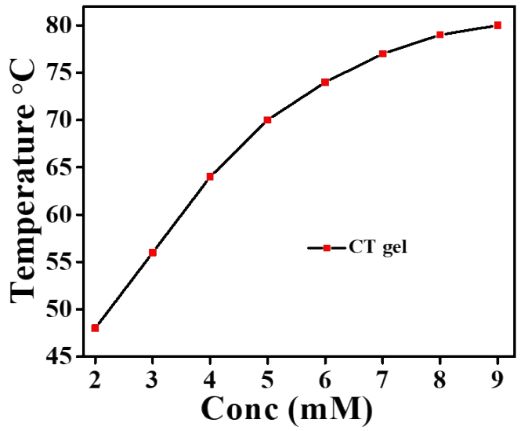

(b)

PyHisOH/ NBD-Ox (6 mM)	State	T_{gel} (°C)
1:0.5	Gel	45
1:0.75	Gel	53
1:1	Gel	74
1:1.5	Weak gel	-
1:2	Viscous	-

Figure S2. (a) Concentration dependent gel melting temperature (T_{gel}) of CT hydrogel. (b) Gel melting temperature of CT hydrogel at different concentration of acceptor (**NBD-Ox** = 0.5-2 mM) at fixed

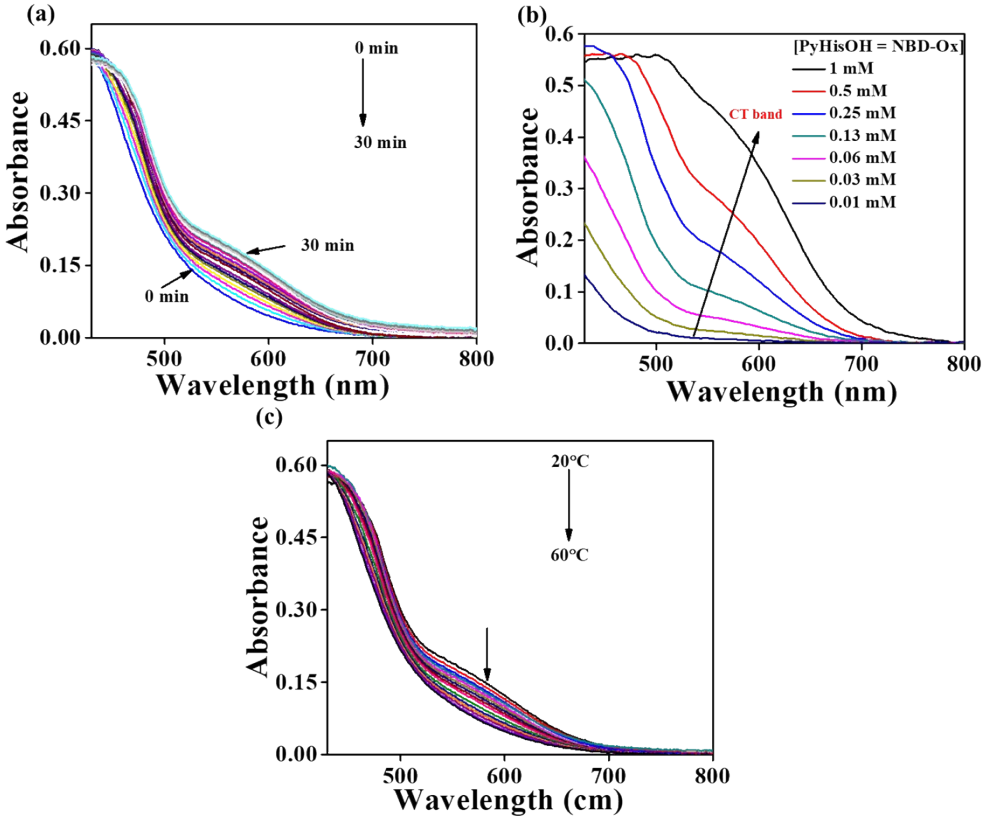

concentration of donor (**PyHisOH** = 6 mM).

Figure S3. (a) Time dependent absorption spectra of 1:1 **PyHisOH**: **NBD-Ox** hydrogel [**PyHisOH** = **NBD-Ox**] = 0.25 mM in PBS buffer of pH 7.4. (b) Concentration dependent absorption spectra of 1:1 **PyHisOH**: **NBD-Ox** (0.01-1 mM) hydrogel in PBS buffer of pH 7.4. (c) Temperature dependent absorption spectra of 1:1 **PyHisOH**: **NBD-Ox** hydrogel. [**PyHisOH** = **NBD-Ox**] = 0.25 mM in PBS buffer of pH 7.4.

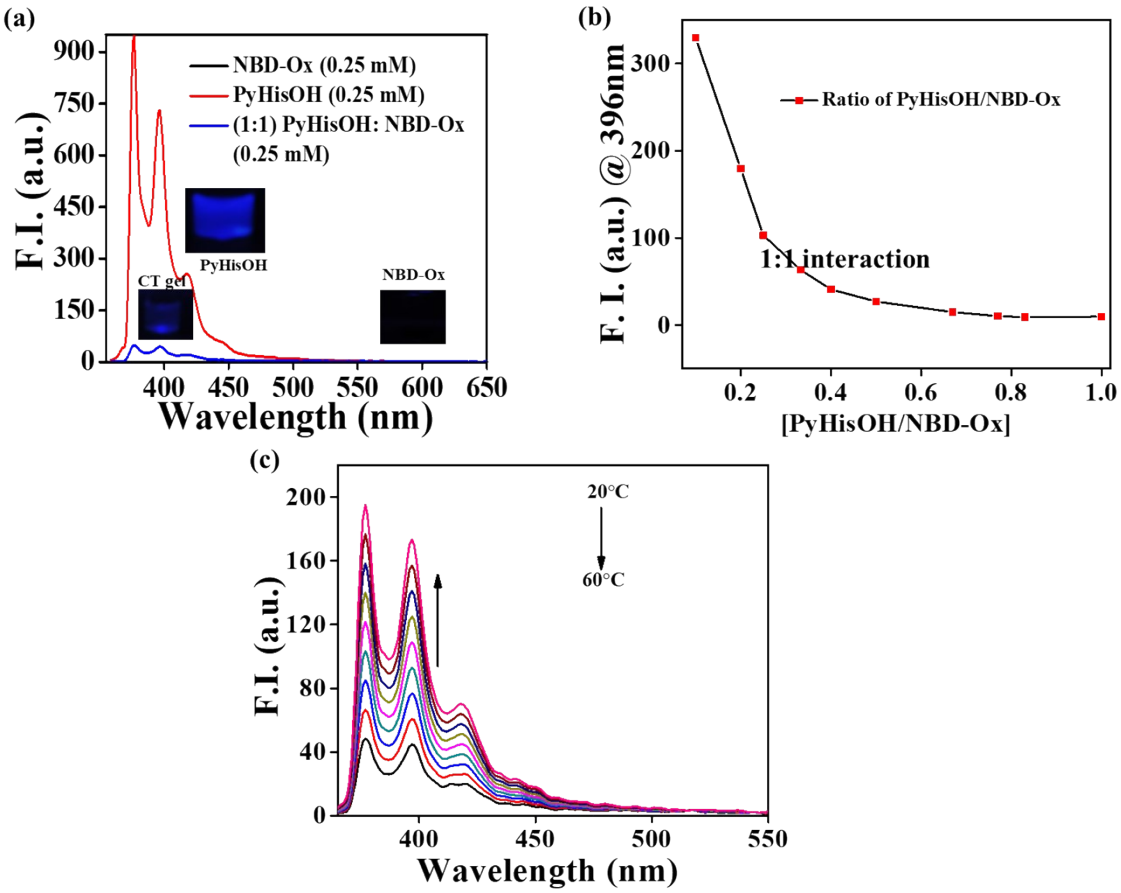

Figure S4. (a) Comparative emission spectra of **PyHisOH** (0.25 mM, λ_{ex} = 345 nm), **NBD-Ox** (0.25 mM, λ_{ex} = 385 nm) and CT hydrogel (0.25 mM, λ_{ex} = 345 nm) in PBS buffer of pH 7.4. (b) Jobs plot for the interaction of 1:1 **PyHisOH** and **NBD-Ox**. (c) Temperature dependent emission spectra of 1:1 **PyHisOH**: **NBD-Ox** hydrogel. [**PyHisOH** = 0.25 mM, λ_{ex} = 345 nm] in PBS buffer of pH 7.4.

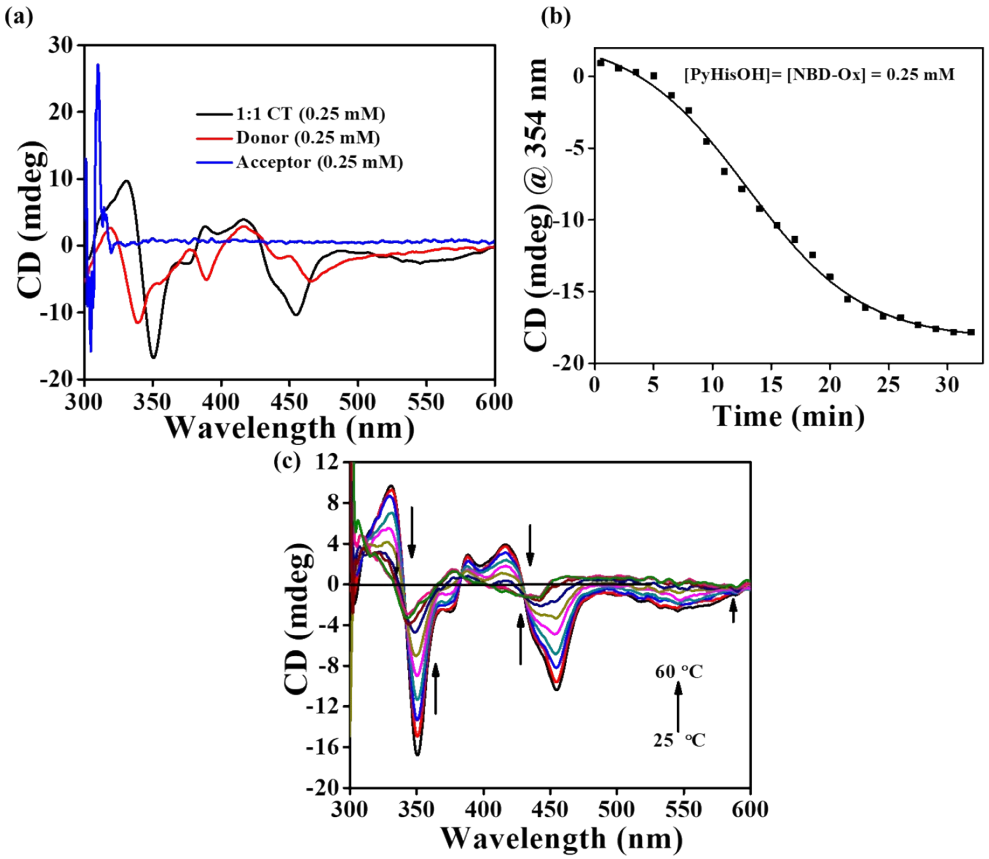

Figure S5. (a) CD spectra of **PyHisOH** (0.25 mM), **NBD-Ox** (0.25 mM) and 1:1 **PyHisOH**: **NBD-Ox CT** hydrogel (0.25 mM) in PBS buffer of pH 7.4. (b) Time dependent CD spectra of 1:1 **PyHisOH**: **NBD-Ox** hydrogel at 354 nm, [**PyHisOH = NBD-Ox**] = 0.25 mM in PBS buffer of pH 7.4. (c) Temperature dependent CD spectra of 1:1 **PyHisOH**: **NBD-Ox** hydrogel, [**PyHisOH = NBD-Ox**] = 0.25 mM in PBS buffer of pH 7.4.

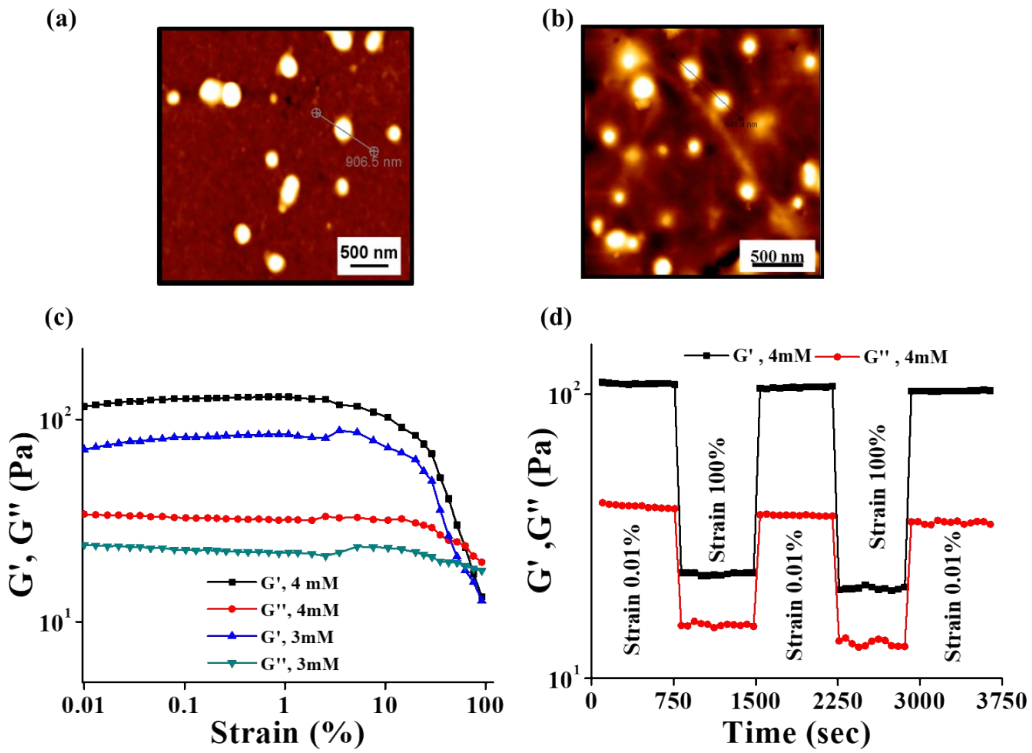

Figure S6. AFM images of (a) donor (0.06 mM). (b) acceptor (0.06 mM). (c) Concentration dependent Oscillatory amplitude sweep rheology data of 1:1 **PyHisOH**: **NBD-Ox CT** hydrogel (3 mM and 4 mM) in PBS buffer of pH 7.4. (d) Step strain experiment for 1:1 **PyHisOH**: **NBD-Ox CT** hydrogel (4 mM) in PBS buffer of pH 7.4.

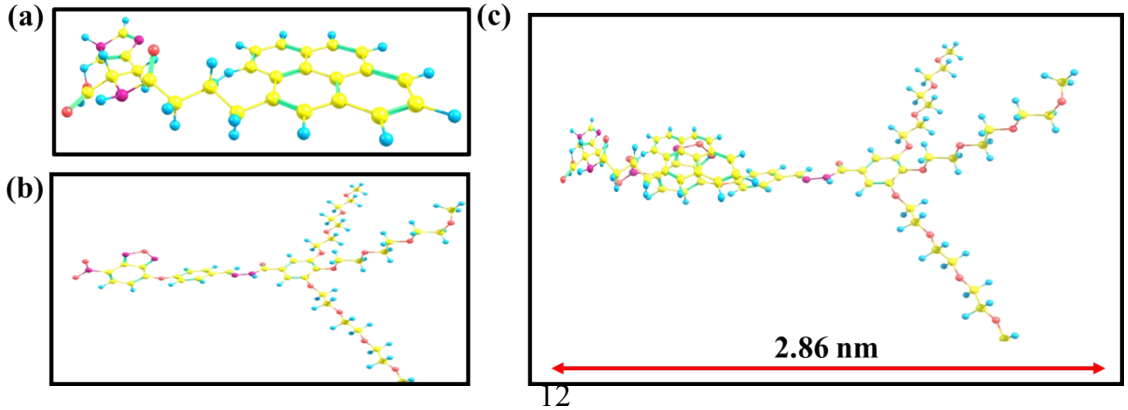

Figure S7: Energy minimized structure of (a) **PyHisOH**, (b) **NBD-Ox,** and (c) 1:1 **PyHisOH: NBD-Ox** based on B3LYP/6-31G* level of computational.

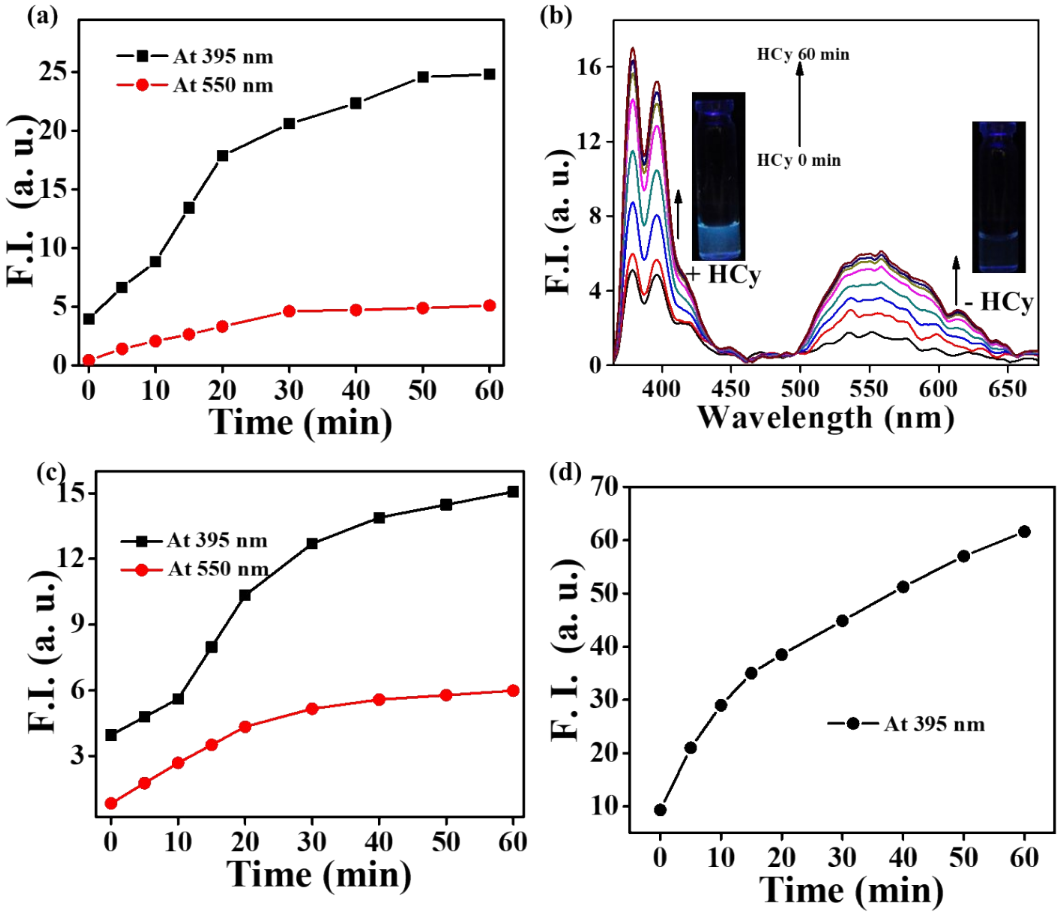

Figure S8. (a) Change in the emission intensity of **PyHisOH**: **NBD-Ox** complex (**PyHisOH** = **NBD-Ox** = 0.25 mM, λ_{ex} = 345 nm) at 395 nm and 550 nm on interaction with Cysteine in PBS buffer of pH 7.4. (b) Time dependent interaction of 1:1 **PyHisOH**: **NBD-Ox** complex (**PyHisOH** = **NBD-Ox** = 0.25 mM, λ_{ex} = 345 nm) with Homocysteine (5 mM) in PBS buffer of pH 7.4. (c) Change in the emission intensity of **PyHisOH**: **NBD-Ox** complex (**PyHisOH** = **NBD-Ox** = 0.25 mM, λ_{ex} = 345 nm) at 395 nm and 550 nm on interaction with Homocysteine (5 mM) in PBS buffer of pH 7.4. (d) Change in the emission intensity of **PyHisOH**: **NBD-Ox** complex (**PyHisOH** = **NBD-Ox** = 0.25 mM, λ_{ex} = 345 nm) at 395 nm on interaction Glutathione (5 mM) in PBS buffer of pH 7.4.

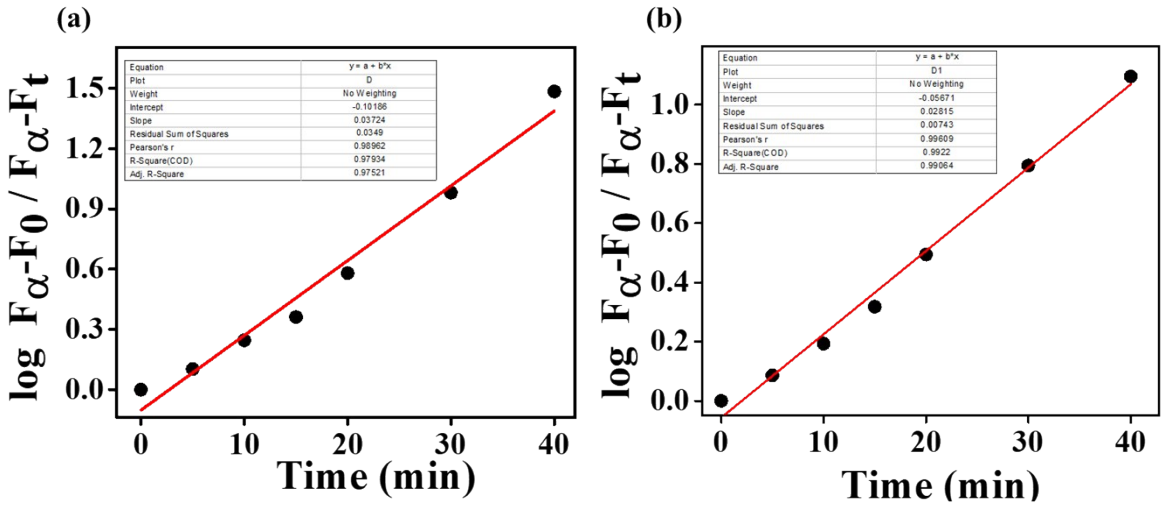

Figure S9. Rate constant calculation for the interaction of 1:1 **PyHisOH**: **NBD-Ox** complex (**PyHisOH** = **NBD-Ox** = 0.25 mM) with (a) Cysteine (5 mM), (b) Homocysteine (5 mM) using pseudo 1st order equation.

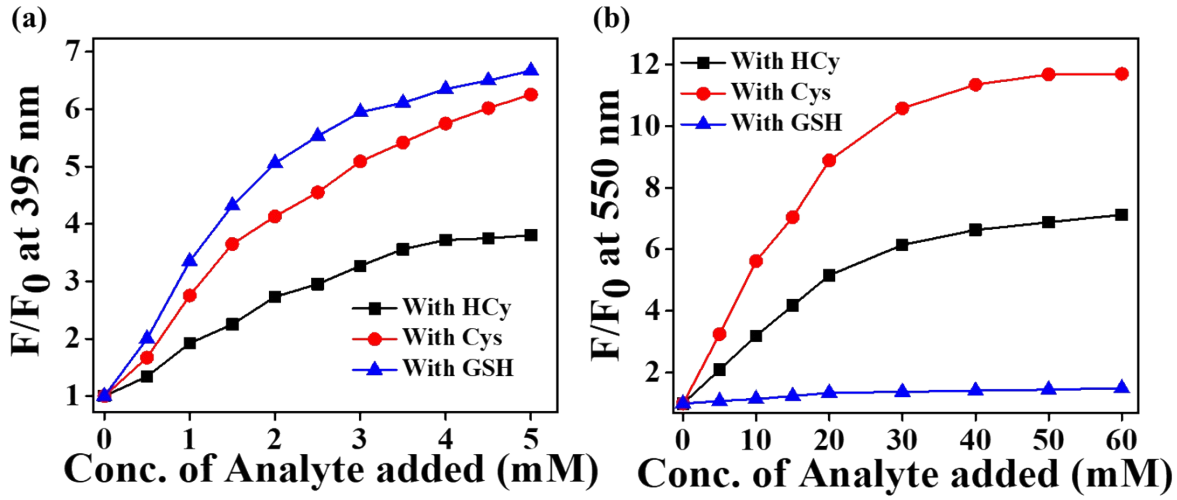

Figure S10. Concentration dependent emission spectra for the interaction of 1:1 **PyHisOH**: **NBD-Ox** complex (**PyHisOH** = **NBD-Ox** = 0.25 mM) with, Cysteine (0-5mM), Homocysteine (0-5 mM) and Glutathione (0-5 mM) at (a) 395 nm, (b) 550 nm in PBS buffer of pH 7.4.

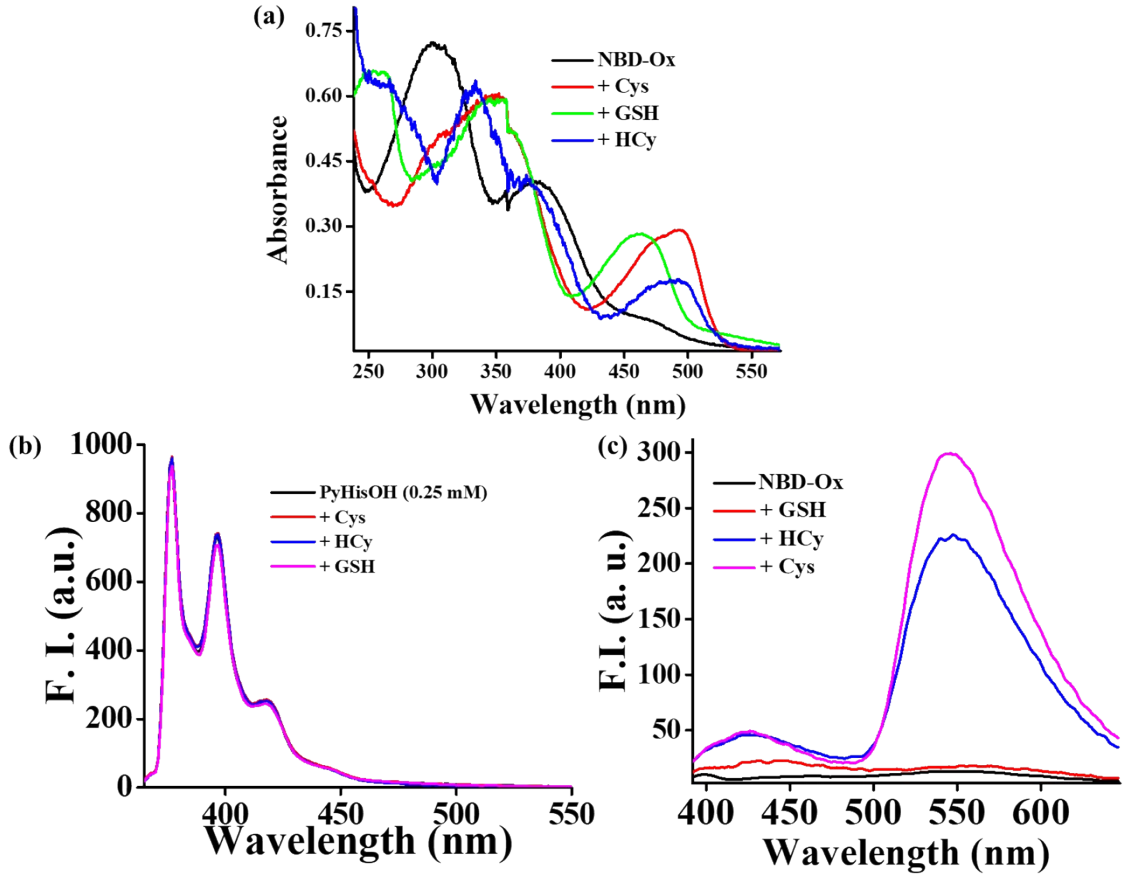

Figure S11. (a) Absorption spectra for the interaction of **NBD-Ox** (0.25 mM) with different analyte (Cysteine, Homocysteine and Glutathione) in PBS buffer of pH 7.4. Emission spectra for the interaction of (c) **PyHisOH** (0.25 mM, λ_{ex} =345 nm) (d) **NBD-Ox** (0.25 mM, λ_{ex} = 385 nm) with different analyte (Cysteine, Homocysteine and Glutathione) in PBS buffer of pH 7.4.

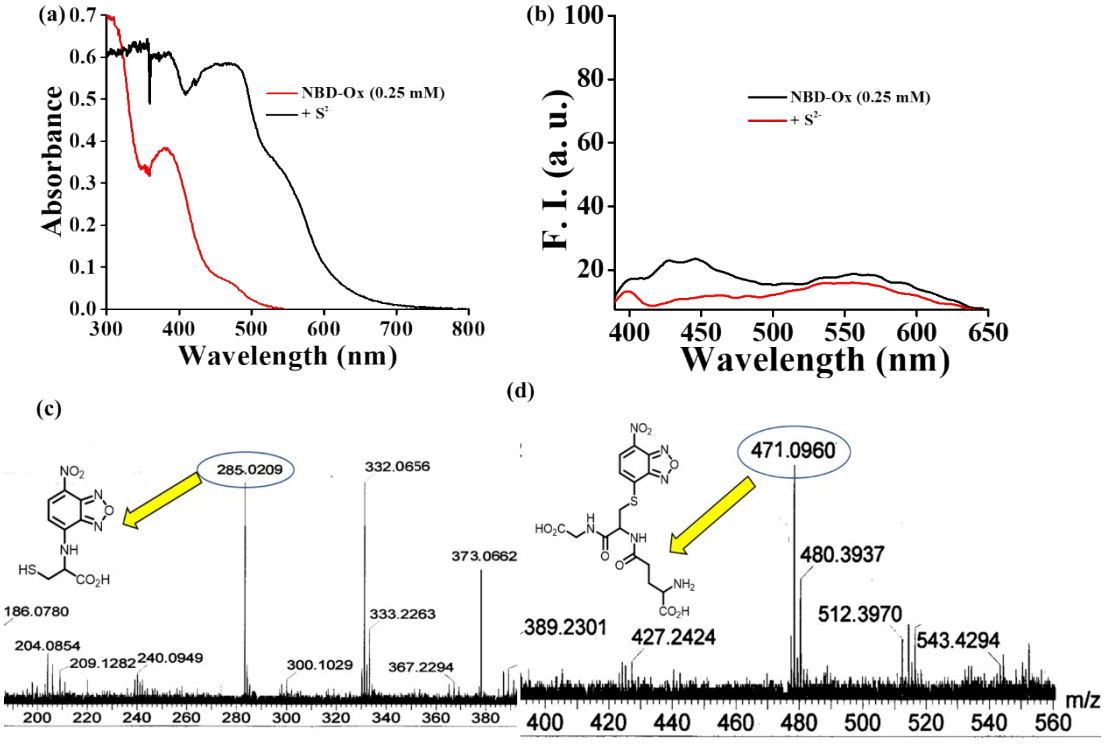

Figure S12: (a) Absorption and (b) Emission spectra for the interaction of **NBD-Ox** (0.25 mM, λ_{ex} = 385 nm) on interaction with Na_2S in PBS buffer of pH 7.4. ESI-Mass spectra for the adduct formation of (c) Cysteine and (d) Glutathione on interaction with 1:1 **PyHisOH**: **NBD-Ox** complex.

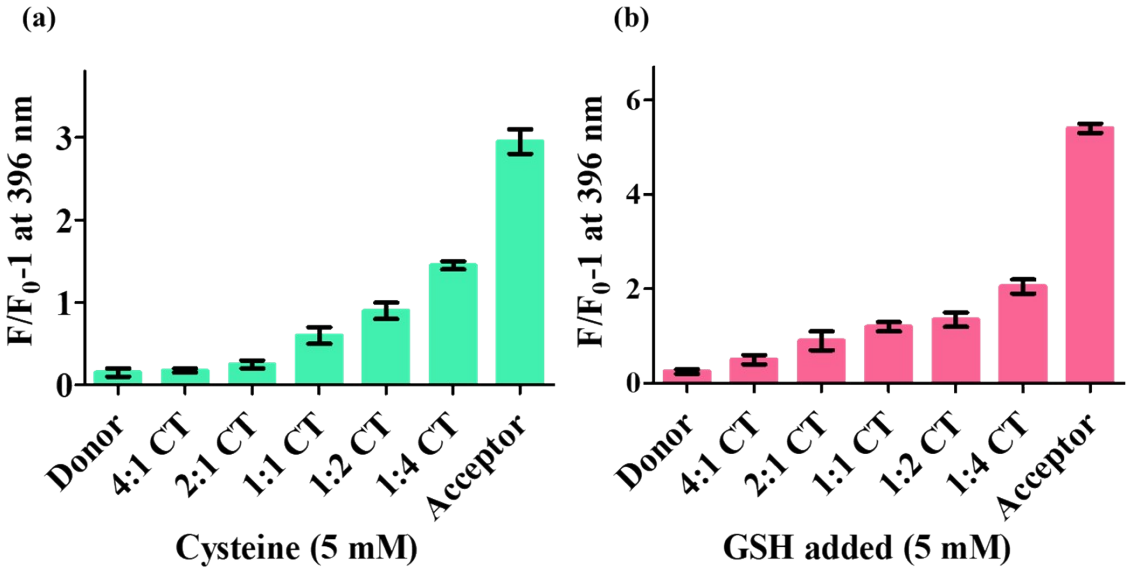

Figure S13. Emission spectra for the interaction of (a) Cysteine and (b) Glutathione with increasing concentration of **NBD-Ox** (λ_{ex} =345 nm) in PBS buffer of pH 7.4**.**